Probing the quenching effect in CsI for high-energy particles

Benoit Lott (CENBG) and Frederic Piron (GAM)

17th September 2004

This short note summarizes the different steps leading to the determination of the quenching factors from the GSI data and discusses the results.

1 Description of the analysis

The analysis was carried out both at CENBG and GAM with the same procedure but different softwares. The main difference lay in the event selection applied. The reaction events were fairly effectively rejected in the GAM analysis, by requiring that one and only one crystal was hit per layer, with a signal above the pedestal greater than three times the pedestal width. No such attempt was performed in the CENBG analysis.

1. The initial EM and FRS data (in "ced" and "lmd" formats respectively) were merged into a single ROOT TTree using the program GlastGSI written by Denis Dumora, each set constituting a separate branch. The TTree only contains raw data.

2. The EM pedestals were extracted by Frederic using the early GSI test runs in which the EM was externally triggered by a pulser. The purpose of these runs was to check the synchronization of the EM and FRS data streams. As no signal was present at the ADC level, these runs are well suited for the pedestal determination. The pedestal peaks were fitted with a gaussian function. A comparison with values obtained earlier at SLAC showed a small systematic difference of about 4 channels in the peak means. This difference may be due to an ADC drift.

3. The non-linearity correction for all 4 ranges per log was performed using Sasha's algorithms and coefficients, as obtained from the charge-injection measurements.

4. The absolute energy calibration for the LEX8 ranges was established by adjusting the measured deposited-energy distributions obtained for 1.7 GeV protons to the corresponding distributions predicted by GEANT4

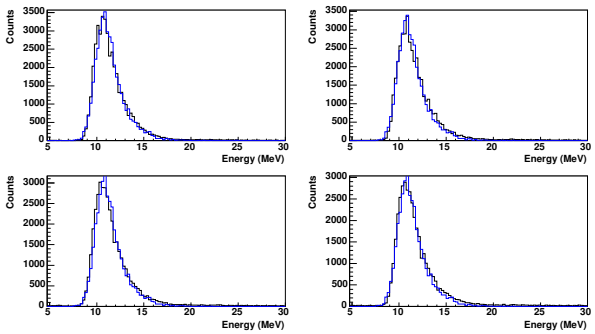

Figure 1: Calibrated deposited-energy distributions for 1.7 GeV protons (black histograms) compared to the corresponding GEANT4 predictions, spread by 0.6 MeV (blue histograms), for the first four EM layers.

(Fig.1). The latter distributions had to be smeared with a gaussian distribution of width 0.6 MeV to better reproduce the experimental data[1]. The procedures followed at CENBG and at GAM were slightly different: the adjustment between the two distributions was done directly in the first case, while in the second, the two distributions were separately fitted with Landau distributions, and the relative conversion factors were derived from the fit results. Only a limited number of crystals were hit by protons at GSI: only the columns X=3, X=6 and Y=6 , Y=9 have been considered in the analysis so far. Most calibration coefficients found in the two analyses are consistent within 2%, with a maximum difference of 4%.

5. Cross-calibration between different energy ranges for the same log was performed by comparing the data measured in the overlapping regions (about 600 ADC channels - out of 4095- for the upper range) of adjacent ranges. Multiplying the LEX8 calibration coefficients by the so-obtained relative factors provided successively the calibration coefficients for LEX1[2], HEX8 and HEX1 (Figs 2&3). These coefficients were compared to those extracted using "cosmic" muons by Sasha: they are systematically found slightly lower (between 2 and 5%) than Sasha's. This systematic effect results most probably from differences in the reference distributions considered in the various analyses, for cosmic muons (NRL) and 1.7 GeV protons (CENBG & GAM).

6. The quenching factors, defined as the ratio between measured and theoret-

[1] The need for this smearing was initially found in the analysis of the CERN data obtained for high-energy muons with the minical.

[2] For LEX1 on the X layers, the preamp reset was erroneously disabled during the experiment, causing a loss of correlation for some events as visible as a cloud of points and a secondary line on the left-hand panels of Fig. 2.

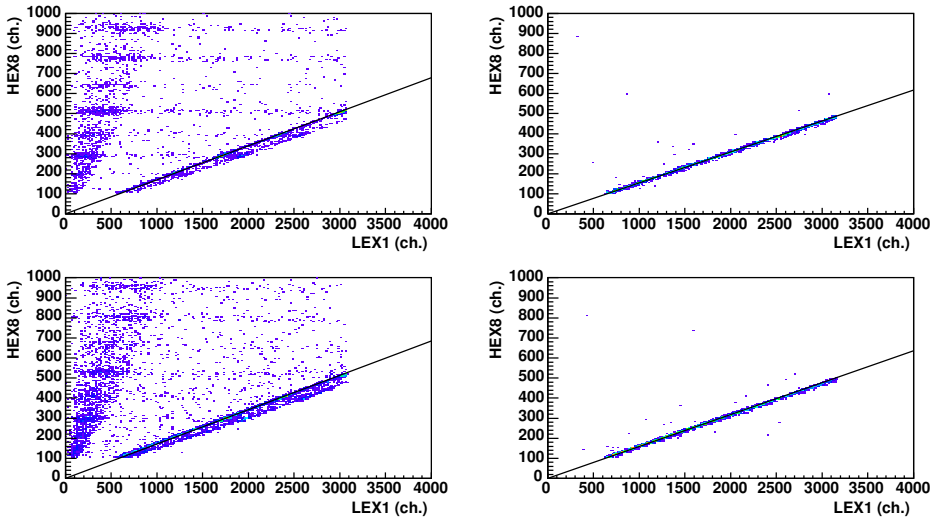

Figure 2: Correlation between LEX1 and HEX8 data measured for some logs in the first four layers, fitted either with the newer version of ASICs (left panels) or with the older version (right panels).

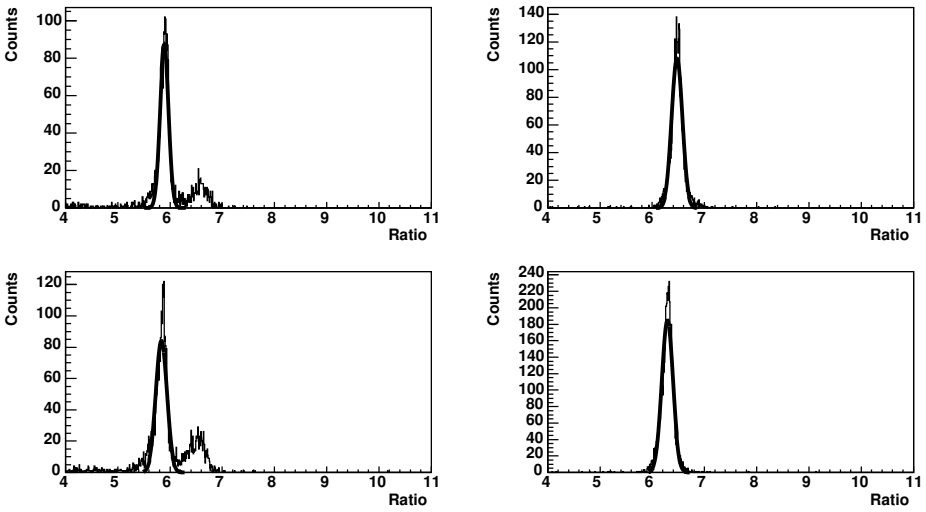

Figure 3: LEX1/HEX8 ratios corresponding to the data presented in the preceeding figure.

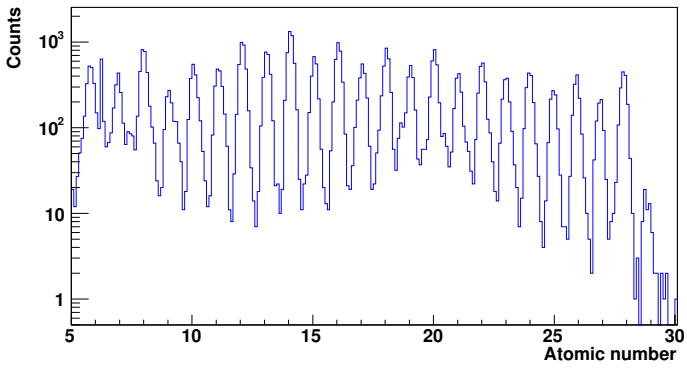

Figure 4: Atomic number distribution of ions as measured by the FRS ionisation-chamber MUSIC for the cocktail-beam runs.

ical deposited energy, were obtained for the various incident ions through the following steps.

- The incident ions were selected by using the information from the FRS ionisation chamber MUSIC (Fig.4), duly calibrated (the calibration changed as a function of time, since for a given ion, the signal amplitude scaled with the chamber gas pressure, which was at atmospheric pressure).
- The ionisation-energy peaks were fitted with gaussian functions in the ion-selected histograms (Fig. 5). The fit was performed independently for each end of the log. For the X layers, the ratio of the two means varies significantly with the ion Z, manifesting the lateral dispersion of the ions along the focal plane caused by the spectrometer and stemming from the light tapering. This dependence is illustrated in Fig. 6 for the first layer. The average of the two energies was considered in the rest of the analysis to be insensitive to this effect.
- The resulting mean energies obtained for the different ions were then compared with those extracted from the GEANT4 simulations in a similar fashion (Fig. 7).

For light, high-energy ions, the measured energies are found *higher* than the calculated energies, by 23% for C, corresponding to an *antiquenching* effect (see below). This effect can be tracked down to lower energy thanks to the 1 GeV/nucleon data, as some ions approach or reach full stopping in the calorimeter (Fig. 8). For example, a gradual transition towards the expected quenching behavior is observed for Z=15 ions as the ions slow down.

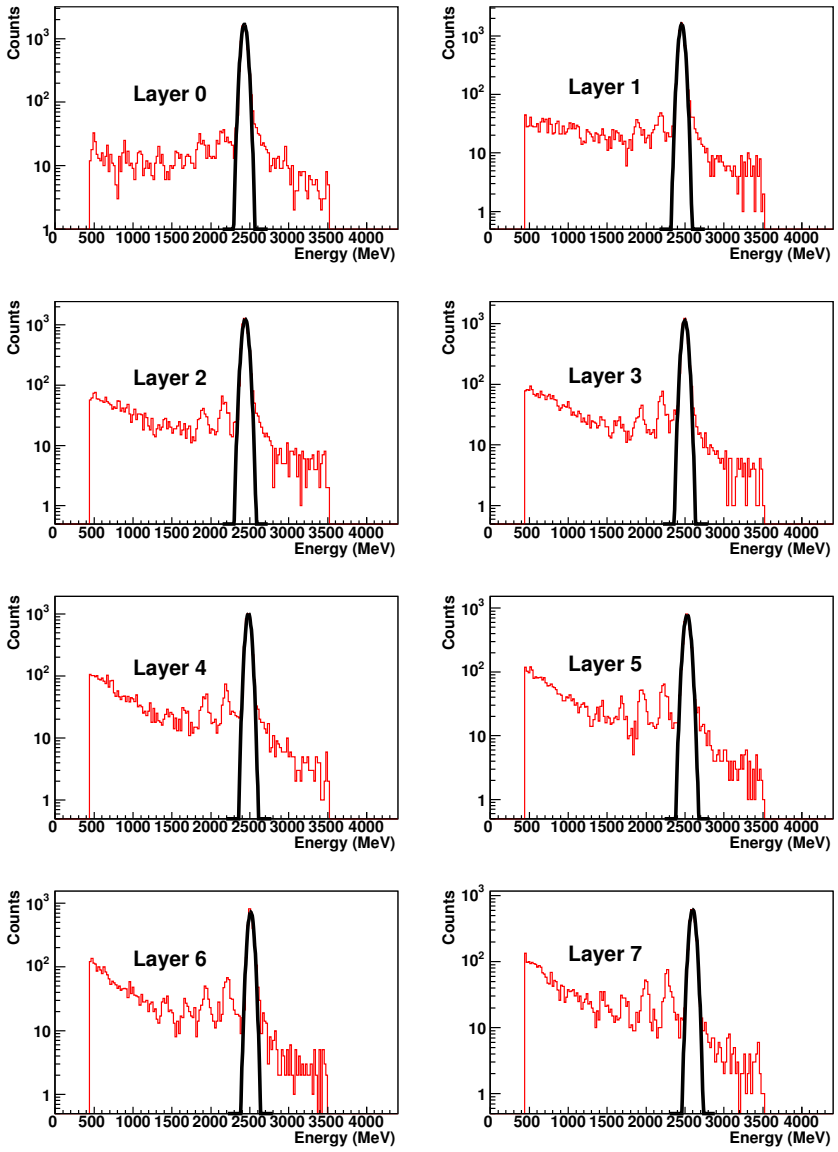

Figure 5: Deposited-energy distributions measured in the eight EM layers for 1.7 GeV/nucleon Si ions. The black curves correspond to the gaussian fits of the ionization peaks. The secondary peaks at lower energy correspond to charge-changing events in which the primary ions lost 1, 2, 3, ..., protons.

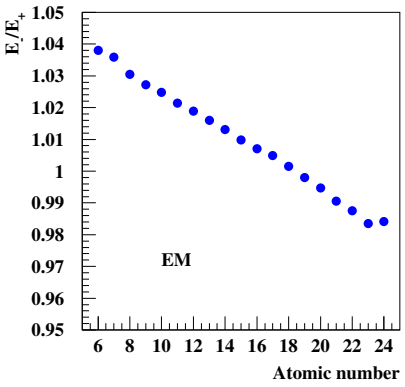

Figure 6: Ratio of the mean energies measured at the two ends of a log in the first layer, as a function of the ion atomic number.

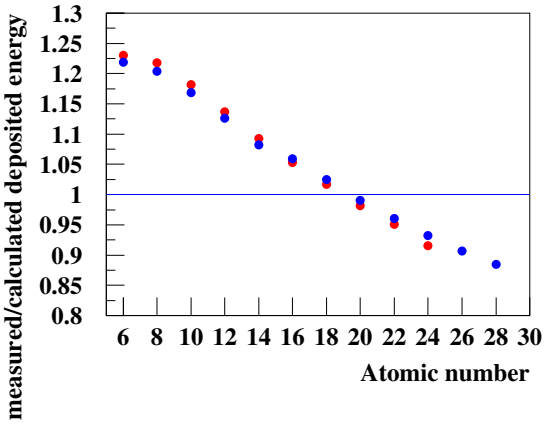

Figure 7: Ratio of mean measured/ calculated deposited energies as a function of the ion atomic number. The red (blue) dots correspond the EM (minical) data. The beam energy is 1.7 GeV/nucleon.

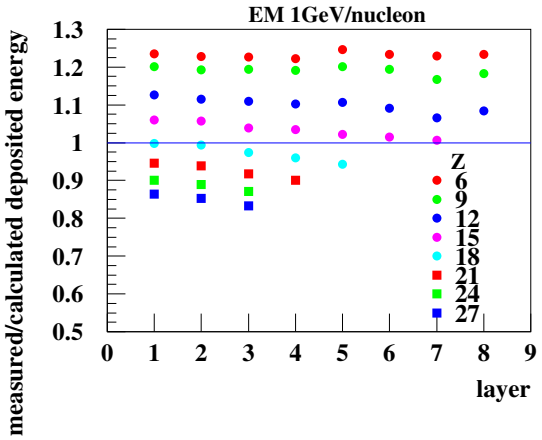

Figure 8: Ratio of mean measured/ calculated deposited energies as a function of the EM layer for different ion atomic numbers. The beam energy is 1GeV/nucleon.

2 Discussion of the results

Since this effect is unexpected, it is worthwhile to go through the different checks which have been applied either on the data or the simulation results. The results have proved robust so far against these checks.

First of all, the good agreement between minical and EM results (Fig. 7) seems to rule out an electronics-related problem, since the minical makes use of peak-sensing ADCs while the EM ASICs sample the analog signals at a fixed delay time through a Track&Hold stage. Many electronics checks concerning the pedestals and the energy calibration for the minical were carried out at CENBG and an excellent consistancy with the beam data was obtained.

The absolute energy calibration derived from the proton data was checked (for the minical) using gamma-rays from a ^{22}Na source. Good agreement between the different calibration coefficients (MeV/ ADC units, within 2% and 8% for the two tested logs) was observed. For the minical, the calibration established at GSI using 1.7 GeV protons was also compared to that established at CERN with 20 GeV muons for the same crystals. Again, the agreement was found to be excellent. It must be emphasized that the longitudinal shower profiles measured at CERN and calibrated with the above procedure were found in good agreement with the GEANT4 predictions[3] (Fig.9), demonstrating the

[3]The GEANT4 simulations have still to be improved, as part of the upstream material was not taken into account.

particle	BB	SRIM	NIST	G3 v3.21	G4 v5.2	G4 v6.0
proton	0.571	0.572	0.580	0.556	0.554	0.546
Carbon	20.58	20.26	n.a.	20.18	20.14	20.04

Table 1: Energy loss in MeV/mm for 1.7 GeV/nucleon proton and Carbon as calculated with different models.

validity of the calibration procedure, the correct energy assignment to the muon ionization peak and justifying the implicit assumption that there is no quenching for muons or protons [4].

Another possibility may be that the deposited energies calculated by GEANT4 are incorrect. Other calculations [1]were carried out with different programs: SRIM[2], NIST[3], GEANT3, different versions of GEANT4, or by simply integrating the Bethe-Bloch formula. The results, displayed in Table 1 for C and protons respectively and different incident energies show little dispersion. The reference results given by SRIM are 1% and 4% higher than the GEANT4 predictions for Carbon ions and protons respectively. Please note that using the SRIM results would actually *increase* the amplitude of the anti-quenching effect.

Can the anti-quenching be real, i.e. due to a physical process at play in the scintillator? Quenching is understood as resulting from the excitation of non-radiative degrees of freedom in the scintillator because of the high ionization density arising from the passage of a large-Z ion, bringing about a non-linear light function $L(\Delta E)$, where ΔE is the energy deposited within the crystal. At low energy, the effect only depends on dE/dx (Birks' Law[4]) but at high energy, it also becomes dependent on the ion Z: at a fixed dE/dx, the higher Z, the higher β and thus the greater the δ-electron emission, reducing the quenching[6][5]. Since dE/dx decreases and the fraction of the energy carried by δ-electron increases as the particle energy increases, both factors concur to a reduction in quenching at higher energy.

Quenching is not observed for electrons, i.e. $L(\Delta E)$ is linear and dL/dE is constant. Although it is not trivially obvious, quenching is apparently also absent for high-energy protons and muons. With the reference scale adopted in the analysis, no quenching corresponds to $dL/dE = 1$, the "classical" quenching situation corresponds to $dL/dE < 1$, and antiquenching to $dL/dE > 1$.

It is instructive to compare the quenching factors measured at GSI with those obtained[5] at GANIL below 73 MeV/nucleon (Fig.10). The latter experiment was performed with the same crystals, PIN diodes as at GSI and the minical electronics and the data were analysed with a similar procedure (the ions being stopped inside a crystal, the quantity $L(E)$ was actually measured, dL/dE being

[4] Although we are dealing with a degenerate case, the accidental cancellation of the effects resulting from two or more of these hypotheses being wrong seems unlikely.

[5] Due to their long ranges, δ electrons escape the primary ionization column and leave their energy in a less dense ionization region.

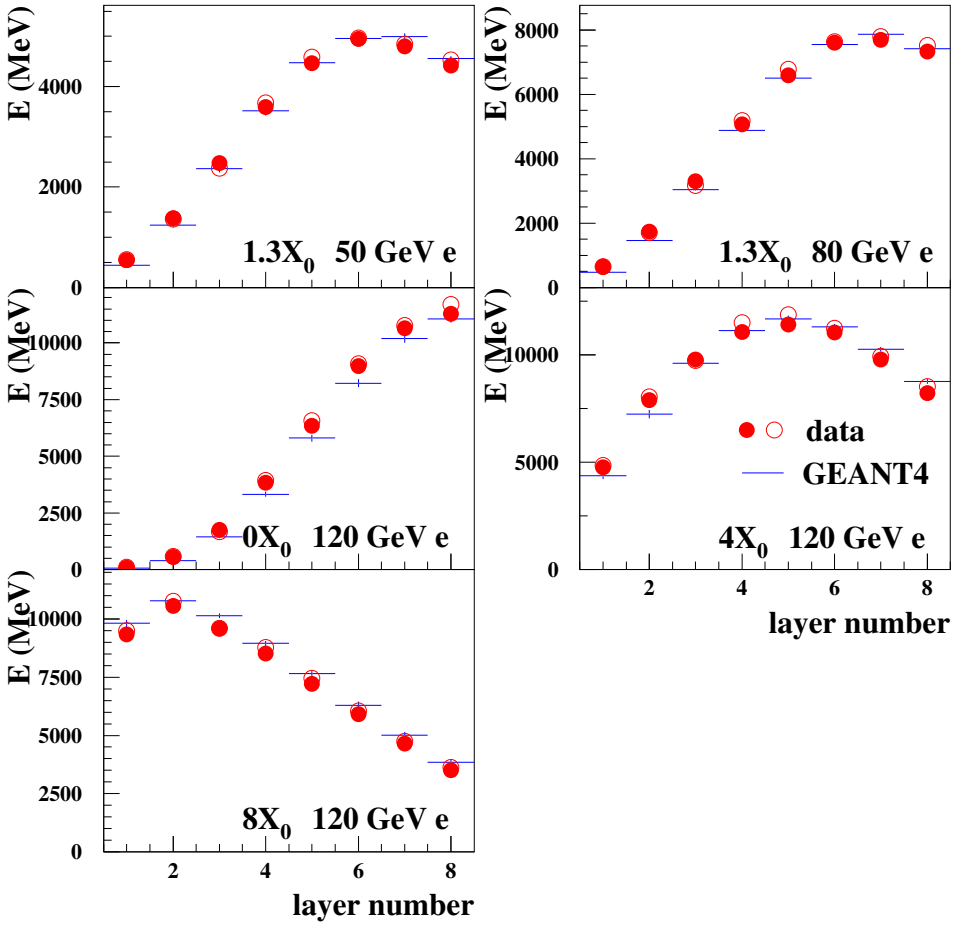

Figure 9: Longitudinal profiles measured at CERN (dots) compared to the GEANT4 predictions (bars), for different electrons energies and thicknesses of the upstream Pb block.

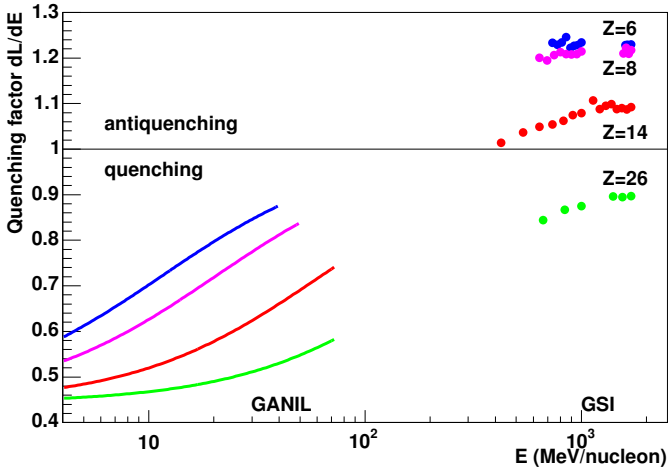

Figure 10: Compilation of the quenching factors measured at GANIL and GSI as a function of the ion's energy per nucleon, for the different ions relevant to the on-orbit calibration of GLAST's calorimeter.

derived by differentiation of the functionals fitted on the data). At low energy, the expected quenching situation ($dL/dE < 1$) indeed prevails but the quenching factors rise with the ion energy, as expected. The GSI data fall rather nicely in the trend of the GANIL data.

From Fig.10, antiquenching is thus not as suprising as it may first appear.

How can heavy ions give rise to more light *being measured* than protons do, at a given ΔE ? The answer may lie in the time dependence of the light output, observed to be different between protons and heavier nuclei. The light output can be described as the sum of two exponential functions associated with a fast and slow component:

$$L(t) = \frac{h_f}{\tau_f}\exp(-\frac{t}{\tau_f}) + \frac{h_s}{\tau_s}\exp(-\frac{t}{\tau_s})$$

Fast and slow components arise from the deexcitation of different states of the scintillator[7]. The fast component corresponds to the radiative capture by Tl activator sites of loosely bound electron-hole pairs (excitons), whose formation is favored at high ionization density. On the other hand, the slow component arises from the capture of individual electrons and holes resulting in the excitation of metastable states not accessible to excitons.

Experimentally, it was found[8] below 30 MeV/nucleon that $\tau_s \simeq 7\mu s$ and remains essentially constant for all particles whereas $\tau_f \simeq 0.5\text{-}1\mu s$ and varies significantly with the particle nature. The slow component represents more than 30% of the total light yield for protons and increases with the particle energy[8],

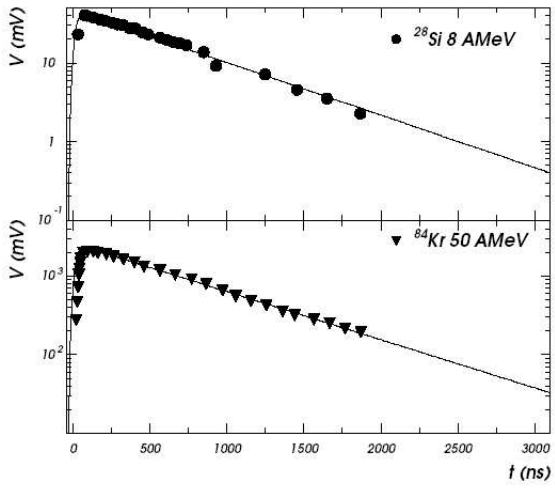

Figure 11: Temporal pulse shapes for low-energy ions, measured with a phototube. The curves are the results of a fit with an exponential function with $\tau = 0.65\mu s$ (from ref. [6]).

while it is almost negligible for heavy ions. The latter feature is illustrated in Fig.11 , displaying the pulse shape measured with a phototube for low-energy heavy ions: only one component, having a decay time of 650 ns, is present. This difference in pulse shapes between protons and heavier particles is commonly used at low energy (E<100 MeV/nucleon) for particle identification.

How do these components evolve in the energy domain relevant to GLAST? Since we make use of charge preamplifiers, it is not possible to directly measure $L(t)$, but the voltage pulse at the preamplifier output (Fig. 12) corresponds to the integral over time of $L(t)$ folded with the preamp exponential decay ($RC_f = 93\mu s$ for the minical preamp). Fitting this pulse with the appropriate function yields: $\tau_f = 1.27 \pm 0.04\mu s$, $\tau_s = 10.0 \pm 0.7\mu s$, $\frac{h_s}{h_s+h_f} = 25 \pm 1\%$ for cosmic muons (the uncertainties are statistical, an average being carried out over an ensemble of 15 pulses). The slow and fast contributions along with their sum are depicted in Fig. 12. τ_s is found to change notably for different pulses, with a distribution extending between $5\mu s$ and $15\mu s$. The present findings confirm the evidence for a slow component of comparable magnitude observed[9] by the BELLE collaboration and associated with a time constant of $\tau_s = 17\mu s$.

Because of its fairly short shaping-time constant (3.5 μs), the ASIC amplifier filters out the slow component almost completely, while leaving the fast one less affected. This is illustrated by the results of a toy calculation producing the voltage pulses output by the amplifier for different decaying times, the total

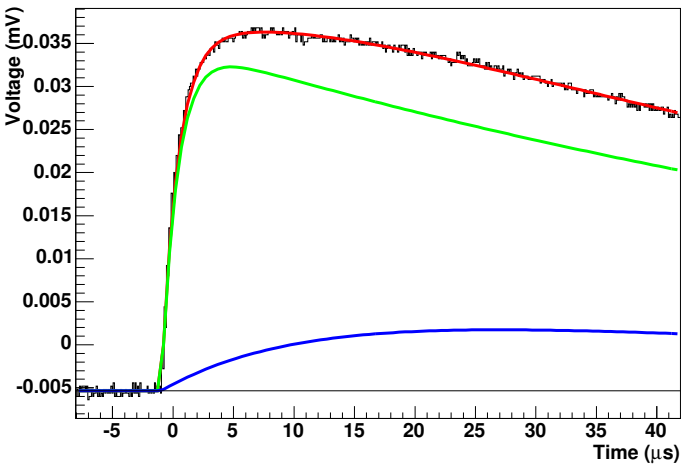

Figure 12: Experimental voltage pulse at the preamplifier output for a cosmic muon (the detector and electronics are from the minical). The curves correspond to the results of the fit described in the text. The green (blue) curve corresponds to the contribution of the fast (slow) component, and the red one to their sum.

charge being constant (Fig.13)[6]. The difference in pulse shapes between protons and heavy-ions, if it still prevails at high energy, could thus give rise to the observed "antiquenching" effect.

Is any direct evidence for this effect present in the GSI data? The "TACK optimization" runs, in which the amplitude was scanned as a function of the delay time applied to the pulse sampling, do reveal a subtle change in pulse shapes for different beam particles, as displayed in Fig.14 (a scan to longer times would have been useful for the present purpose). Though the change in amplitude is only a few percent, this observation seems to support the present hypothesis. A noticeable difference exists between Carbon ions and heavier ones in Fig.14, implying that a slower component would not be totally absent for light ions, in the scope of this hypothesis.

Further data could help settle this issue definitively. A short measurement

[6]The voltage is the inverse Laplace transform of:

$$L(s) \quad = \quad \frac{Q}{1+\tau_1 s} \times \frac{1}{C_f s} \times \frac{\tau s}{(1+\tau s)^2}$$

where the first term on the rhs corresponds to the exponential decay of the input charge, with integral Q, the second to the transfer function of the charge-preamp, $C_f$being the feedback capacitor value, and the last to the transfer function of the shaping amplifier taken for simplicity as a CR-RC circuit with a single time constant τ. The preamp decaying time has not been considered for simplicity.

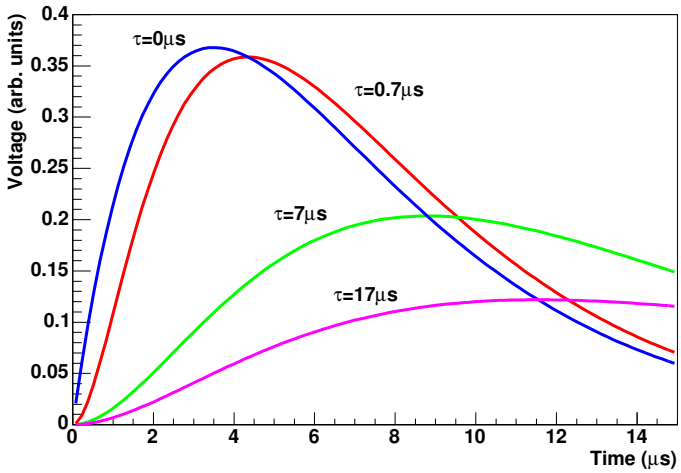

Figure 13: Calculated voltage pulses at the shaping-amplifier output for different charge pulses applied to the preamp input, with the following time dependence: a δ-function and three exponential decays exp(-t/τ), assuming a shaping time of 3.5 μs.

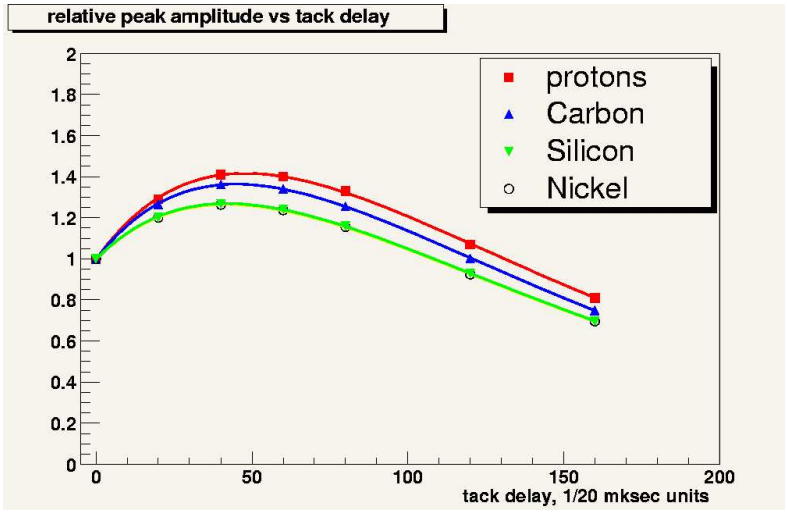

Figure 14: Pulse shape for different beam particles, as measured in the "tack optimization" runs at GSI. From Sasha Chekhtman.

of the pulse shape for 800 MeV Carbon ions at GSI, either directly with a photomultiplier [7]or at the charge preamp output, as illustrated in Fig. 12, would be valuable in this respect. Unfortunately, this measurement does not seem to be feasible in a near future because of the poor prospects to get beam time at GSI.

Let us summarize the proposed explanation for the behavior of the quenching factors displayed in Fig. 10. If there was not quenching (meant here as related to the intrinsic property of CsI) at all, the very fact that part of the energy goes into the slow component for protons and a lesser part for ions would lead to an observed-antiquenching case, as the slow component is essentially filtered out by the shaping amplifier. At low energy, this behavior is masked as (intrinsic) quenching is very strong for heavy ions and overbalances this effect. As the ion energy increases, quenching is reduced and the antiquenching case eventually prevails, at least for light ions.

Whatever explanation holds, the quenching factors obtained at GSI (Fig. 8) can be used for the in-flight calibration as long as they can be safely extrapolated to higher energies, 90% of the cosmic-ray ions having an energy in the range 1.5 - 10 GeV/nucleon according to CREME[10]. The quenching-factor dependence on the ion energy is actually found to be negligible between 1.0 and 1.7 GeV/nucleon (Fig. 10), while $\frac{dE}{dx}$ varies by 7% in this range. Although a thorough error calculation is still to be done, at the present stage of the analysis it can be expected that the quenching-factor uncertainty associated with the measurement and the extrapolation to the energy domain relevant to Glast should end up close to 3%.

References

[1] Th. Reposeur, "Note on the energy loss by ionization: GEANT 4 status".

[2] http://www.srim.org/SRIM/SRIM2003.htm

[3] http://physics.nist.gov/PhysRefData/Star/Text/programs.html

[4] J.B. Birks, Theory and Practice of Scintillation Counting (Pergamon, 1964).

[5] J. Bregeon, PhD thesis, in progress.

[6] M.Parlog et al., Nucl. Instr. and Meth. A 482 (2002) 674.

[7] W.R. Leo, Techniques for Nuclear and Particle Physics Experiments (Springer Verlag, 1994).

[8] F. Benrachi et al., Nucl. Instr. and Meth. A 281 (1989) 137.

[7]although $\frac{h_s}{h_s+h_f}$could be found to be different if the spectral distributions of the two components don't match, since the spectral sensitivities of the PIN diodes is markedly shifted as compared to that of a PM.

[9] B. Shwartz, private communication to S. Chekthman and Preprint physics/0403136.

[10] A. J. Tylka et al., "CREME96: A Revision of the Cosmic Ray Effects on Micro-Electronics Code", IEEE Transactions on Nuclear Science, 44, 2150-2160 (1997).